Journal of Photochemistry and Photobiology A: Chemistry 214 (2010) 194–202

Contents lists available at ScienceDirect

Journal of Photochemistry and Photobiology A: Chemistry

journal homepage: www.elsevier.com/locate/jphotochem

Effect of V-UV-radiation on VOCs-saturated zeolites

José Biomorgi[a,b], Esther Oliveros[a], Yves Coppel[c], Florence Benoit-Marquié[a,*], Marie-Thérèse Maurette[a]

[a] Laboratoire des IMRCP, UMR CNRS 5623, Université Paul Sabatier (Toulouse III), 118 rte de Narbonne, 31062 Toulouse Cédex 9, France
[b] PDVSA-Intevep, Urbanización Santa Rosa, Sector El Tambor, Los Teques, Estado Miranda, Apartado 76343, Caracas 1070A, Venezuela
[c] Laboratoire de Chimie de Coordination, UPR CNRS 8241, 205 Route de Narbonne, 31077 Toulouse Cédex 04, France

ARTICLE INFO

Article history:
Received 7 April 2010
Received in revised form 18 June 2010
Accepted 24 June 2010
Available online 3 August 2010

Keywords:
Zeolite
VOCs
Adsorption
Photochemical gas treatment
Solid-state NMR

ABSTRACT

The combination of adsorption on zeolites and vacuum ultraviolet (V-UV) irradiation was applied to the treatment of gaseous effluents containing volatile organic compounds (VOCs). A xenon-excimer (Xe_2^*) radiation source emitting at 172 nm was employed and two types of zeolites (faujasite Y (DAY) and ZMS-5 (DAZ)) were tested in adsorption/irradiation cycles of three model VOC pollutants (1-butanol, benzene and toluene). A specific diffusion cell was used in dynamic experiments for producing air streams containing each VOC at chosen and stable concentrations. Scanning electron microscopy (SEM) and X-ray photoelectron spectroscopy (XPS) analyses were performed on the solids after VOC saturation and irradiation. Important changes were detected in the properties of the DAY zeolite when using toluene as a pollutant. In particular, the Si/Al ratio was modified at the surface and in the framework of the zeolite, as a consequence of a rearrangement of the Al and Si atoms in the solid. In contrast, the DAZ zeolite retained its superficial and structural properties after V-UV treatment. In the case of 1-butanol, changes in the zeolite structure were negligible, and no change was observed in the zeolite in the case of benzene. Solid state NMR analysis confirmed these results and revealed that when the DAY zeolite saturated with toluene was irradiated at 172 nm, changes in the shifts of Si and Al atoms took place, suggesting a possible interaction/reaction between the zeolite framework and the benzyl radical produced as a consequence of the toluene oxidation.

1. Introduction

Volatile organic compounds (VOCs) are major air pollutants coming largely from industrial processes. One of the procedures available for the treatment of gaseous effluents containing low levels of pollutants involves usually two-steps: adsorption of pollutants onto a porous material and regeneration of the adsorbent by pollutant degradation [1,2]. During the last two decades, developments in air and water treatment have led to an improvement of techniques for the oxidative degradation of organic pollutants, in particular with the application of photochemical methods, generally referred to as Advanced Oxidation Processes (AOP). A large attention has been devoted to photocatalytic processes, using primarily titanium dioxide (TiO_2, generally anatase phase) as a photocatalyst [3], often supported on bulk materials such as SiO_2, zeolites and activated carbon. The use of zeolites as photocatalyst support is especially interesting due to their high adsorption capacity and thermal and structural stability. Zeolites with faujasite structure including zeolites Y (Si/Al > 1.5) and X (Si/Al ≤ 1.5) are of great interest because of their various applications in industrial processes. In particular, zeolite molecular sieves are widely applied in conventional catalysis and adsorption/separation processes. Zeolite molecular sieves have also been employed as supports of photocatalysts for water treatment [4–10] and, to a lesser extent, for air treatment [11,12]. However, little attention has been devoted to the potential role of the zeolites themselves (*e.g.* as photocatalysts). Recently, Kato et al. [13] reported that HZSM-5 and hydrogen type mordenite exhibit a photocatalytic activity for non-oxidative coupling of methane under UV irradiation in the wavelength range of 200–270 nm, suggesting that Al–O units in the zeolite framework were the photocatalytic active sites. Yan et al. [14] found that commercial raw HZSM-5 zeolites showed good activities for photocatalytic oxidation of organic compounds in an air stream under irradiation at 254 nm. However, their photocatalytic activity was dependent on the content in iron oxides and the zeolite itself did not appear to be involved.

We previously reported [15] the use of vacuum-ultraviolet (V-UV) irradiation at 172 nm to regenerate a commercial zeolite which was used as a pollutant reservoir to adsorb aliphatic VOCs (1-butanol and methyl ethyl ketone). Complete mineralization of 1-butanol and methyl ethyl ketone could be achieved, with a very good concomitant regeneration of the adsorbent in both cases. However, the potential effect of the V-UV radiation on the zeolite

---

* Corresponding author. Tel.: +33 05 61 55 69 68; fax: +33 05 61 55 81 55.
E-mail address: florence@chimie.ups-tlse.fr (F. Benoit-Marquié).

1010-6030/$ – see front matter © 2010 Elsevier B.V. All rights reserved.
doi:10.1016/j.jphotochem.2010.06.026

Table 1
Main properties of adsorbents used in this work.

Symbol	Crystalline type (pore structure)	Available porous volume ($cm^3\,g^{-1}$)	Channels diameter (Å)	Surface area ($m^2\,g^{-1}$)
DAY	Faujasite Y (α-cage)	0.37	7.4	680
DAZ	ZSM-5 (interconnected channels)	0.17	5.6	330

structure was not investigated and the method was not tested on aromatic pollutants.

In this work, we have investigated the effect of V-UV irradiation on the degradation of volatile organic compounds (VOCs) contained in gaseous effluents and adsorbed on zeolites. 1-Butanol, benzene and toluene were used as models for aliphatic and aromatic pollutants, respectively. Two types of zeolites were employed as adsorbents: faujasite Y (DAY) and ZMS-5 (DAZ). Cycles of adsorption/irradiation were performed, using a xenon-excimer lamp as a V-UV (172 nm) continuous radiation source. During the dynamic experiments performed, the gaseous effluent was analyzed on-line at the exit of the photochemical reactor by gas chromatography (GC) and Fourier transform infrared spectroscopy (FT-IR). Moreover, the effects of V-UV irradiation on the properties and structure of the zeolites themselves and when saturated with pollutant were investigated. In order to further investigate the role of the zeolites in the VOCs degradation process, several analytical techniques were employed: solid state nuclear magnetic resonance (ssNMR), X-ray photoelectron spectroscopy (XPS), Brunauer–Emmett–Teller analysis (BET) and scanning electron microscopy (SEM).

2. Experimental

2.1. Materials

1-Butanol (99.5%), benzene (99%) and toluene (99%) were purchased from Aldrich, and used as received. The commercial zeolites used in this study were cylindrical pellets (diameter 2 mm, length 5 mm) supplied by Degussa. Both granular solids were made of microcrystals of zeolites arranged together with the same clay binder and in the same proportion (20% weight). Table 1 summarizes the adsorbent main properties.

2.2. Characterization of zeolites

The zeolites were characterized by the following methods: solid state nuclear magnetic resonance (solid state NMR), X-ray photoelectron spectroscopy (XPS), BET surface area measurements (BET) and scanning electron microscopy (SEM) coupled with an EDX detector.

Solid-state NMR spectra were recorded on a Bruker Avance 400 spectrometer equipped with a 4 mm probe operating at 399.60 MHz for ^{1}H, 104.12 MHz for ^{27}Al, and 79.39 MHz for ^{29}Si. Samples were spun at 12 kHz at the magic angle using ZrO_2 rotors. All chemical shifts for ^{29}Si and ^{27}Al are relative to TMS and 1 M $Al(H_2O)_6{}^{3+}$ solution, respectively. For ^{27}Al MAS (magic angle spinning), single pulse experiments at small flip angle (15°) were used with a recycle delay of 3 s. ^{29}Si CP/MAS (cross-polarized/magic angle spinning) spectra were recorded with a recycle delay of 5 s and a contact time of 3 ms. ^{29}Si MAS spectra were obtained under high-power proton decoupling conditions; a small flip angle (30°) was used, as well as long recycle delays (60 s).

The XPS analyses were carried out using a Leybold–Heraeus commercial surface analysis apparatus (LHS 11), equipped with a single channel detector, and employing AlKα radiation (1486.6 eV) at 360 W (power settings: 12 kV and 30 mA). The 100 mm radius hemispherical analyzer was set in the constant pass energy mode (pass energy = 200 eV).

The surface area and pore volume were measured by N_2 physisorption experiments at 77.4 K, employing the BET method and using a Micromeritics ASAP 2010 equipment, following the standard Brunauer–Emmett–Teller (BET) method. The samples were degassed for 4 h, at 120 °C.

The scanning electron microscope (JSM-840 A, JEOL) was operated at 20 keV, providing information on local properties together with chemical composition of the material activated by electronic bombardment (EDS facility). Prior to analysis, the pellets were coated with gold to ensure conductivity.

2.3. Gas phase adsorption/irradiation experiments

2.3.1. Reactor and radiation source

Both adsorption and irradiation experiments were carried out in a continuous flow annular reactor (length: 15 cm, optical path length: 3 mm, total volume: 60 cm^3). The reactor was equipped with a cylindrical xenon-excimer ($Xe_2{}^*$) lamp emitting at 172 (±14 nm) and positioned in the central axis of the reactor. The lamp was driven by a high voltage power supply (ENI Model HPG-2) with an electrical power of 110 W at 185–190 kHz. The radiant efficiency of the radiation source was approximately 8% (photonic flux: $(8.3 \pm 0.5) \times 10^{18}$ photons s^{-1} determined according to Jakob et al. [17,18]). The fixed bed of zeolites was supported by means of a non-porous quartz cloth inserted in the annular space and, with a typical mass of 2 g, an homogeneous bed height of about 1 cm was obtained.

2.3.2. Production of VOC containing air streams

The polluted air streams used in dynamic adsorption/irradiation experiments were generated with diffusion cells [19,20]. These cells were used to produce gas mixtures of stable VOC concentration for very long periods of time. The diffusion cell reservoir containing the liquid VOC was immersed in a thermoregulated water bath and a 80:20 N_2/O_2 mixture (Air Liquide) continuously flushed the reservoir. The air stream was regulated by a mass flowmeter (Brooks 58505, 10–50 mL min^{-1}). VOC concentrations were controlled by the air flow rate through the cell and the temperature of the liquid VOC, and could be varied in the range between 300 and 5000 mg m^{-3}. In this work, a concentration of 2000 mg m^{-3} was used, unless otherwise indicated. A specific diffusion cell was designed for each VOC. The diffusion rate expressed by the Altshuller and Cohen equation was used for the prediction of the experimental temperature-concentration relation, as in a previous study [19]. The vapor pressure of the liquid was estimated by the Antoine equation, whereas the diffusion coefficient was calculated using the Fuller relation [16]

2.3.3. Adsorption/irradiation experiments

During the adsorption phase, the air stream containing the VOC at a chosen constant concentration passed through the fixed bed of zeolites in the photochemical reactor, while the lamp was off. Once the VOC breakthrough curve was totally described and adsorbent (zeolite) saturation completed (VOC concentration at the exit of the reactor is identical to the entry concentration), the shift from the adsorption to the irradiation/oxidation phase was accomplished by turning the lamp on. The temperature inside the reactor was approximately 40 °C during the irradiations experiments. The anal-

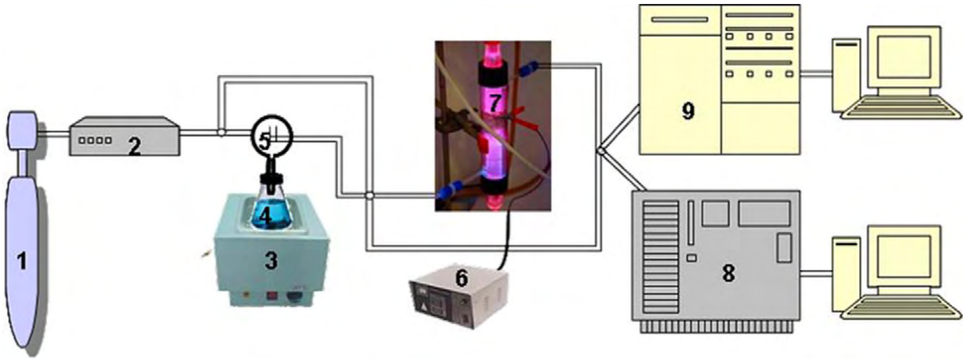

Fig. 1. Schematic experimental set-up (1: N_2/O_2 mixing bottle; 2: flow regulator; 3: thermoregulating bath; 4: liquid VOC; 5: diffusion cell; 6: power supply; 7: annular photochemical reactor equipped with a V-UV lamp; 8: gas chromatograph; 9: infrared spectrograph).

ysis of the reactor outlet was performed on-line using a Chrompack CP900 gas chromatograph, and a Perkin-Elmer 1760-x Infrared spectrograph equipped with a DTGS (deuterated triglycine sulfate) detector for CO_2, O_3 and H_2O detection. For IR analysis, the gas sample continuously flushed a 90 mL NaCl cell. A scheme of the experimental set-up used in this work is shown in Fig. 1.

3. Results

3.1. Adsorption/V-UV irradiation cycles

Two adsorption/V-UV irradiation cycles were performed under a constant flow of an air stream containing a chosen and constant concentration (2000 mg m^{-3}) of VOC (1-butanol, benzene or toluene). The experimental set-up is shown in Fig. 1 and the procedure is described in detail in Section 2.3. As an example, breakthrough curves are represented in Fig. 2 in the case of toluene. The V-UV irradiation was then started and the evolution of the effluent composition at the reactor exit was analyzed by GC as well as by FT-IR. When the amount of VOC reaching the reactor exit was negligible, the lamp was turned off and a second adsorption/irradiation cycle was started.

3.1.1. Toluene degradation

The two adsorption/irradiation cycles in the case of toluene using the DAY zeolite as adsorbent are shown in Fig. 2, the dotted line representing the initial concentration of toluene in the air flow at the entrance of the reactor. During the first 125 h of the adsorption process, toluene was completely adsorbed by the zeolite, which was equivalent to 300 ± 15 mg of pollutant on the 2.132 ± 0.001 g of adsorbent. After this time, the toluene concentration at the reactor outlet increased progressively, and the DAY saturation was reached after 182 h, corresponding to 390 ± 20 mg of toluene adsorbed in the zeolite (equivalent to 2.0 ± 0.1 mmol g^{-1}).

Switching on the V-UV lamp induced a photo/thermodesorption process of toluene from the solid, leading to a significant increase of the toluene concentration in the gas phase for a short period of time (Fig. 3), as observed previously with other VOCs [15].

After about 7 h of irradiation, no toluene could be detected at the reactor outlet, as a result of the photolytic effect leading to the oxidative degradation of the VOC, although the toluene containing air stream was continuously flushed through the reactor during the experiment.

After 12 h of irradiation, the second adsorption process was started and the DAY was completely re-saturated after 109 h, which represents approximately 60% of the time taken for the first saturation. This difference in the adsorption time (and therefore in the amount of toluene adsorbed) could be related to the fact that the adsorbent was not completely regenerated after the first irradiation, toluene and its oxidation products remaining in the solid in significant amounts (see below).

The evolution of toluene oxidative degradation was also followed by FT-IR analysis of the gaseous effluent at the reactor outlet. The result is shown in Fig. 4. The signals of CO_2 (2350 cm^{-1}) and H_2O (3650 and 1600 cm^{-1}) confirm an efficient mineralization process of toluene in the gas phase. There are small signals at ca. 3000 and 1700 cm^{-1} corresponding to intermediates produced during irradiation, which disappeared after approximately 1 h of irradiation. A small signal centered at 1050 cm^{-1} and corresponding to ozone vibration could also be detected (ozone formation is due to V-UV

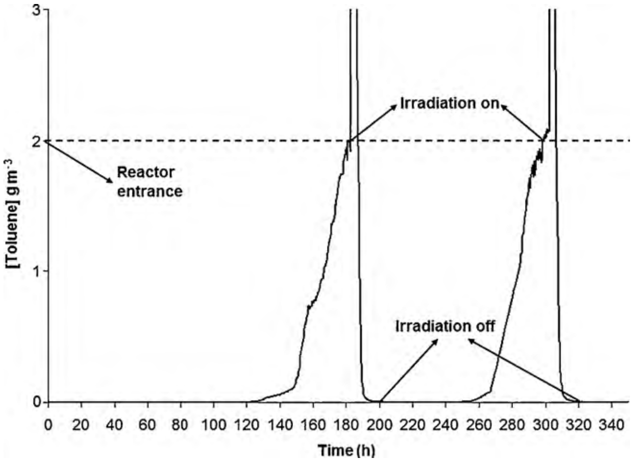

Fig. 2. Adsorption/V-UV irradiation cycles for toluene in the presence of DAY zeolite: variation of the toluene concentration in the gaseous effluent at the reactor outlet as a function of time.

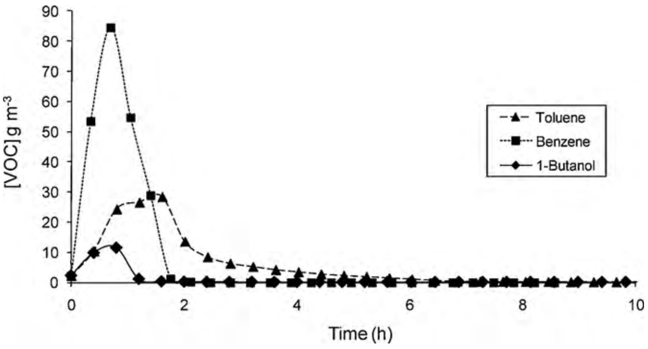

Fig. 3. Evolution of VOCs concentrations in the gaseous effluent at the reactor outlet as a function of the V-UV irradiation time, after saturation of the DAY zeolite with toluene (triangles), benzene (squares) or 1-butanol (circles).

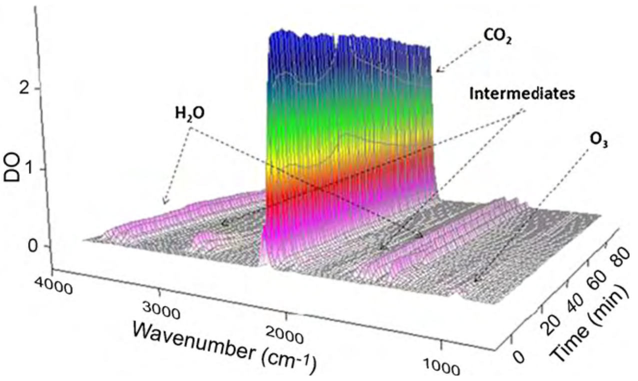

Fig. 4. Evolution of the IR spectrum of the gaseous effluent at the reactor outlet during irradiation at 172 nm, after saturation of DAY with toluene.

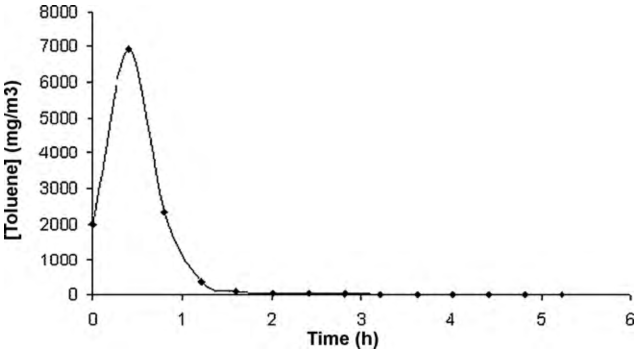

Fig. 6. Evolution of the toluene concentration in the gaseous effluent at the reactor outlet as a function of V-UV irradiation time, after saturation of the DAZ zeolite with toluene.

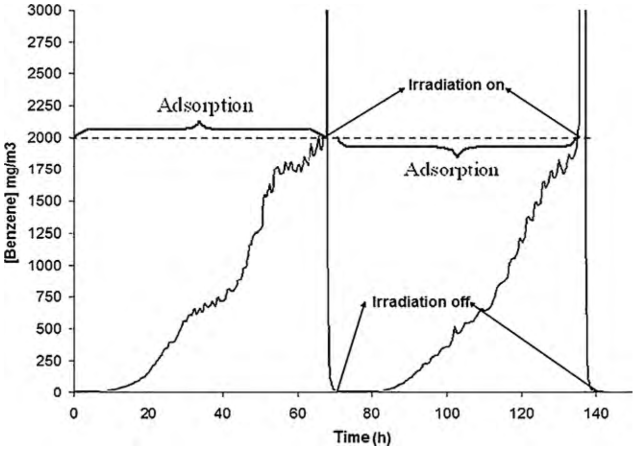

Fig. 7. Adsorption/V-UV irradiation cycles for benzene in the presence of DAY zeolite: variation of the benzene concentration in the gaseous effluent at the reactor outlet as a function of time.

homolysis of O_2 and the reaction of O-atoms thus produced with O_2) [21].

After the adsorption/V-UV irradiation cycles, the DAY pellets were strongly colored (Fig. 5), a phenomenon which was not observed previously with aliphatic VOCs (1-butanol and methyl ethyl ketone [15]). Moreover, the color change was observed inside of the DAY pellets as well as on the surface (Fig. 5).

The most likely explanation of this result is that colored intermediates of the oxidative degradation of toluene remained physically trapped in the zeolite channels and could not be photolyzed and further oxidized. The zeolite could also be involved in the degradation process of toluene, *e.g.* a chemical reaction between the intermediates of V-UV photolysis of toluene, especially C-centered radicals, and the zeolite framework could occur. Changes in the zeolite structure could eventually result from its exposure to the highly energetic V-UV radiation at 172 nm (695 kJ per mole of photons).

In order to evaluate the role of the zeolite structure in the color changes, experiments were carried out with the same pollutant, using a different zeolite adsorbent (DAZ), in otherwise identical experimental conditions.

The evolution of the toluene concentration in the gaseous effluent at the reactor outlet under irradiation at 172 nm, after saturation of the DAZ pellets, is shown in Fig. 6. In this case, only 2 h of irradiation were necessary to obtain a negligible concentration of toluene at the reactor outlet, compared to 7 h in the case of the DAY zeolite. The comparison of the characteristics of both zeolites (Table 1) shows that DAY has a larger available porous volume as well as surface area; consequently, the DAY adsorption capacity is 2.5 times higher than that of DAZ (equivalent to 2.0 and 0.8 mmol g^{-1}, respectively) [22]. These structural properties could be responsible for the differences observed in degradation times when both zeolites saturated with toluene were irradiated. Besides, the DAZ appearance remained almost unchanged after irradiation (data not shown). This observation supports the hypothesis that toluene does not penetrate efficiently inside the channels of DAZ and is degraded under V-UV irradiation in the gas phase and at the zeolite surface. An additional experiment with DAY was carried out, starting the irradiation when the same amount of toluene was adsorbed on DAY as in the case of DAZ. The same color changes in DAY were observed, independent from the toluene concentration, confirming the important role of the adsorbent structure in its regeneration and toluene degradation under V-UV irradiation.

3.1.2. Benzene degradation

The two adsorption/irradiation cycles of benzene, using the DAY zeolite as adsorbent, are shown in Fig. 7. The system behavior was different from the case of toluene: the benzene concentration at the reactor outlet increased already after 5 h and the first saturation of the DAY zeolite was reached after 67 h, which corresponds

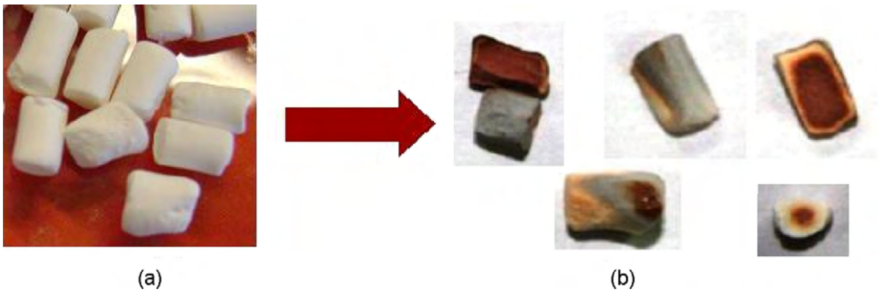

Fig. 5. Pictures of DAY pellets: (a) original and (b) after saturation with toluene and irradiation at 172 nm.

to $1.31 \pm 0.07\,\text{mmol}\,\text{g}^{-1}$. When the lamp was switched on, the V-UV irradiation induced a photo/thermodesorption process from the solid, leading to an increase of the benzene concentration in the airstream for a short period of time (Fig. 3); this increase is important relative to the inlet concentration ($2\,\text{g}\,\text{m}^{-3}$), but corresponds to only approximately 4% of the adsorbed amount. After approximately 3 h of irradiation, the benzene concentration was negligible at the reactor outlet as a result of the photolytic degradation of the VOC. Complete mineralization after 3 h of irradiation was confirmed by performing an on-line FT-IR analysis.

After about 8 h of irradiation, the second adsorption process was started and the DAY was completely re-saturated after 68 h, almost the same time as taken for the first saturation, confirming that a complete and efficient mineralization of the benzene absorbed in the DAY zeolite was obtained after the first irradiation. In contrast to the case of toluene, the aspect of the zeolite pellets remained unchanged after irradiation (data not shown). Apparently, the zeolite was well regenerated under irradiation in this case. The difference observed between toluene and benzene when using the DAY zeolite demonstrates the important role of the CH_3 substituent on the aromatic ring.

3.1.3. 1-Butanol degradation

The results obtained with the aromatic VOCs were compared with those for an aliphatic compound, 1-butanol, using the DAY zeolite as adsorbent. The first saturation of the DAY zeolite was reached after 240 h, and relatively large fluctuations were observed in the adsorption process. This phenomenon has already been described and was the consequence of temperature changes occurring during the day [15,16]. The maximum adsorption capacity of DAY for 1-butanol is $2.6\,\text{mmol}\,\text{g}^{-1}$ [16]. Taking into account this value, it can be expected that 385 mg of 1-butanol was adsorbed in 2 g of DAY zeolite. When starting the V-UV irradiation, similar to toluene, the photo/thermodesorption phenomenon was observed (Fig. 3). After approximately 90 min of irradiation, the 1-butanol concentration at the reactor exit was negligible, a faster degradation than in the case of the aromatic VOCs. The evolution of 1-butanol oxidative degradation was also followed by FTIR and a complete mineralization was obtained.

During the second adsorption process, the re-saturation of the solid needed 152 h, equivalent to approximately 65% of the time necessary to reach the first saturation. However, the adsorption capacity of DAY can be regenerated after V-UV irradiation at 172 nm, as previously reported [15,16]. As in the case of benzene, no color change was detected after irradiation of the 1-butanol saturated DAY.

3.2. Analyses of the zeolites before and after V-UV irradiation

The adsorbents were analyzed using different techniques for checking if changes in the zeolite structure might result from the exposure to V-UV irradiation at 172 nm or if changes required the exposure to both the VOC and the V-UV irradiation.

3.2.1. ^{1}H, ^{29}Si and ^{27}Al solid state NMR

In order to evaluate the effect of VOC adsorbed on the zeolite, solid state NMR analyses were performed on the adsorbent before and after saturation with VOC, as well as after irradiation at 172 nm.

Control experiments showed that V-UV irradiation of the zeolites (DAY and DAZ) at 172 nm for more than 8 h, in the absence of pollutant, did not induce any change in their solid state NMR spectra (^{29}Si CP/MAS, ^{27}Al MAS and ^{1}H MAS).

Representative *^{1}H solid state NMR spectra* are shown in Fig. 8. Several broad signals were observed between 1.0 and 7.0 ppm in the ^{1}H MAS of the original DAY. These NMR resonances have been assigned to different types of OH groups (SiOH, AlOH, bridging SiOHAl, etc.) [23]. Some signals can also be due to physisorbed water molecules.

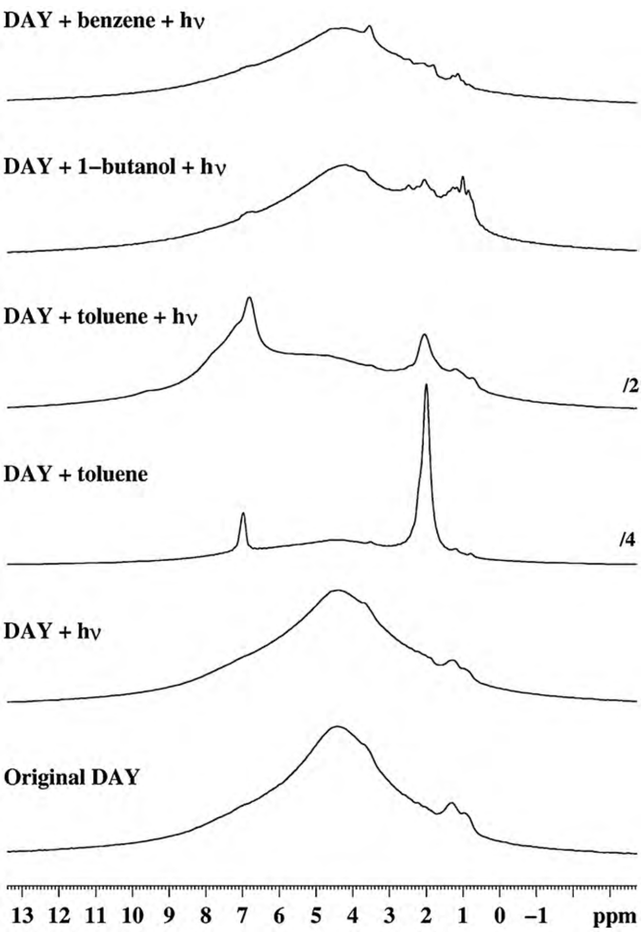

Fig. 8. ^{1}H MAS NMR spectra of original DAY, DAY irradiated in the absence of VOC, DAY saturated with toluene, DAY saturated with toluene, 1-butanol or benzene and irradiated at 172 nm.

When the DAY zeolite was saturated with VOC, besides the signals assigned to the DAY original structure, new signals were observed, as expected: at 2.0 ppm for the ^{1}H of the CH_3 group in the case of toluene and 1-butanol, and at 7.0 ppm for the ^{1}H of the aromatic ring (toluene and benzene).

Clear changes appeared in all cases when the zeolite saturated with a VOC was irradiated at 172 nm (Fig. 8). In the case of toluene, the difference may be attributed to the presence of intermediate compounds produced during the oxidation/degradation process (and remaining initial pollutant not completely degraded). Concerning benzene and 1-butanol, the signals are more diffuse but it appears clearly that the amount of organic compounds remaining in the solid is much lower in comparison to the toluene case. Taking into account the long irradiation time applied to treat the toluene saturated DAY, the organic compounds detected by NMR should be strongly bound inside the zeolite framework.

The *^{27}Al MAS and ^{29}Si CP/MAS NMR* analyses are shown in Fig. 9. The original DAY shows a predominant ^{27}Al MAS signal at 58.4 ppm (Fig. 9a), corresponding to tetrahedral (four-coordinated) framework Al species [24] and a sharp ^{29}Si MAS signal at −107.1 ppm characteristic of highly siliceous zeolite which are assigned to $Si(OSi)_4$, also called Q4 sites [25]. In the ^{29}Si CP/MAS NMR (Fig. 9b), two additional peaks could be detected at −91.1 and −99.6 ppm corresponding, respectively, to Q2 ($Si(OSi)_2(OH)_2$) and Q3 ($Si(OSi)_3(OH)$) site.

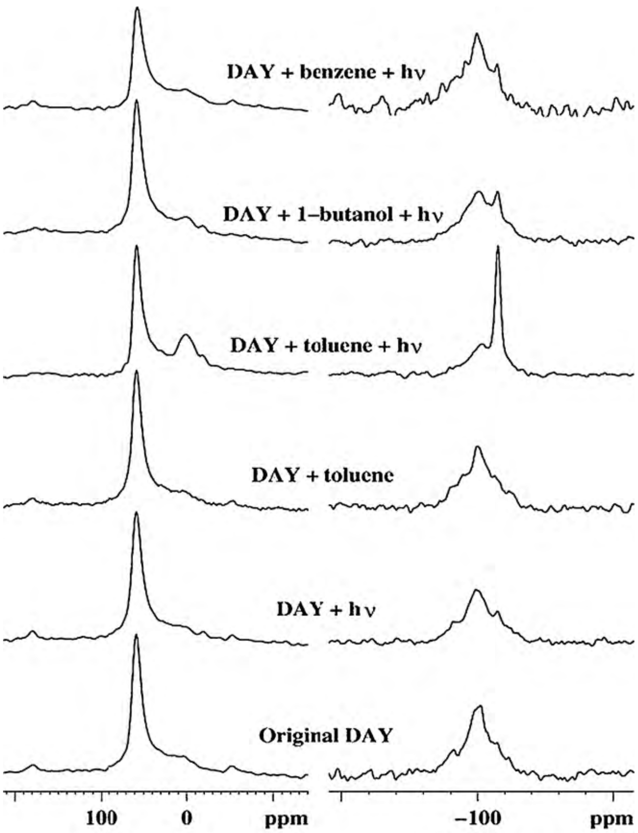

(a) ^{27}Al MAS (b) ^{29}Si CP/MAS

Fig. 9. ^{27}Al MAS and ^{29}Si CP/MAS NMR spectra of original DAY, of DAY irradiated (172 nm) in the absence of VOC, of DAY saturated with toluene, of DAY saturated with toluene or 1-butanol or benzene and irradiated (172 nm).

No change was observed in these spectra when the DAY zeolite was saturated with VOC, confirming that the VOC adsorption in the solid does not produce any change in its Al and Si structure. It also means that the VOC molecules trapped inside the zeolite (observed in the ^{1}H MAS spectrum) are probably highly mobile because no dipolar coupling (average to zero) between the VOC protons and the silicon of the zeolite was detected in the ^{29}Si CP/MAS spectrum.

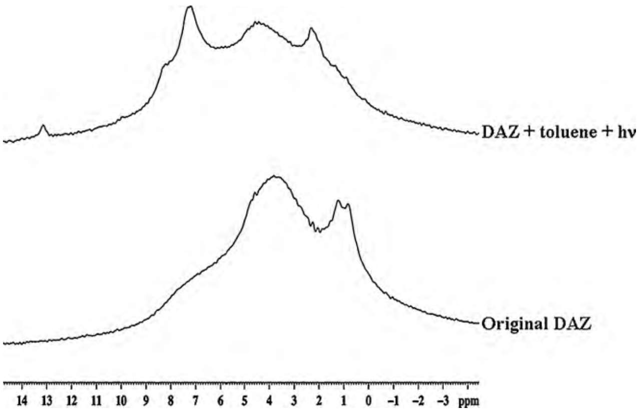

Fig. 10. ^{1}H solid state NMR spectra of original DAZ as well as DAZ saturated with toluene and irradiated at 172 nm.

When DAY was saturated with benzene and irradiated at 172 nm, no change occurred in the ^{27}Al MAS NMR spectrum. However, in the case of 1-butanol and toluene, a new signal could be observed, small in the former case and more pronounced in the latter (Fig. 9a). This signal at 2 ppm could be attributed to six-coordinated extra-framework Al species observed in the dealumination process [24]. In the ^{29}Si CP/MAS NMR spectra, the intensity of the signal of the silicon Q4 site at −107.1 ppm (Fig. 9b) clearly increased after irradiation at 172 nm. This enhancement can be explained by dipolar couplings between Q4 silicons and protons of some of the intermediates compounds produced during the oxidation/degradation process and physisorbed in the zeolite.

Because the most pronounced changes were observed with toluene, solid state NMR analyses were performed with this compound using the DAZ zeolite. The original DAZ shows an ^{1}H MAS NMR spectrum similar to that of the original DAY (Fig. 10). After saturation of DAZ with toluene and irradiation, the ^{1}H MAS NMR spectrum underwent a similar change as observed for DAY. Two additional broad signals at 7.3 and 2.3 ppm were obtained (corresponding to ^{1}H of aromatic and CH_3 group, respectively), showing the presence of remaining toluene and/or degradation products in the DAZ structure. However, according to the relative intensities of zeolite and toluene signals, the amount of VOC remaining in the structure of the DAZ was much lower than in the case of DAY, possibly because the VOC-zeolite interaction was much stronger

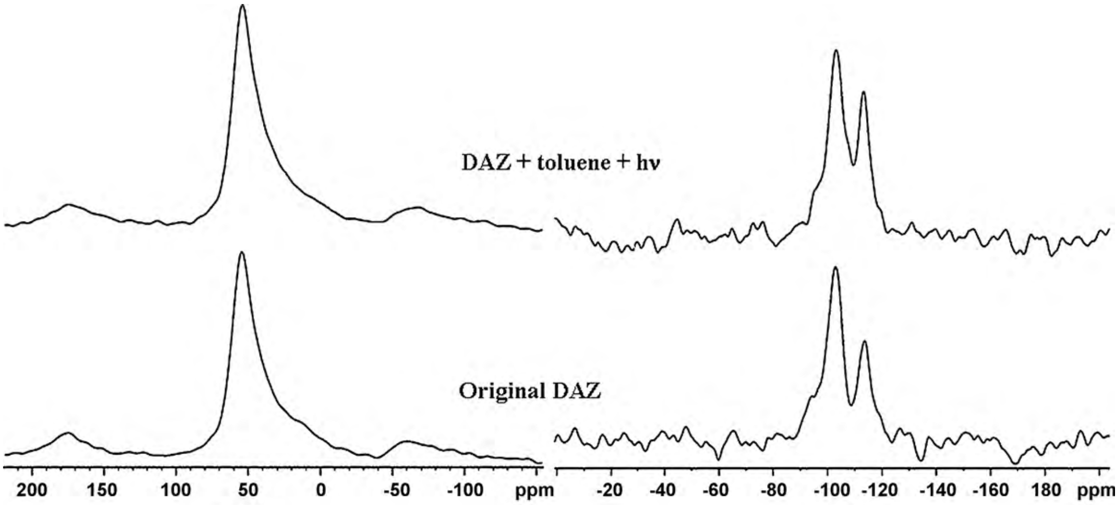

(a) ^{27}Al (b) ^{29}Si

Fig. 11. ^{27}Al and ^{29}Si solid state NMR spectra of original DAZ as well as DAZ saturated with toluene and irradiated at 172 nm.

Table 2
BET analyses of original DAY, DAY irradiated in the absence of toluene, DAY saturated with toluene and irradiated, original DAZ and DAZ saturated with toluene and irradiated at 172 nm.

	Surface ($m^2\,g^{-1}$)	Porous volume ($cm^3\,g^{-1}$)
DAY	680 ± 7	0.37 ± 0.01
DAY + $h\nu$	678 ± 7	0.38 ± 0.01
DAY + Tol + $h\nu$	584 ± 6	0.33 ± 0.01
DAZ	330 ± 3	0.17 ± 0.01
DAZ + Tol + $h\nu$	318 ± 3	0.19 ± 0.01

in the latter case (larger zeolite channels). When DAZ was saturated with toluene and irradiated, in contrast to the case of DAY, no change was observed in the ^{27}Al MAS and ^{29}SI CP/MAS NMR spectra (large ^{27}Al single peak at 54.3 ppm, indicating the presence of four-coordinated extra-framework Al [26]; three ^{29}Si peaks at −96.6, −102.3 and −113.0 ppm assigned to Q2, Q3 and Q4 silicon sites, respectively, Fig. 11).

3.2.2. Physicochemical analyses

3.2.2.1. BET analyses. The BET analyses for DAY and DAZ zeolites are shown in Table 2. The surface areas and porous volumes of DAY remained almost constant when irradiated without pollutant. However, after saturation with toluene and irradiation, both surface and volume decreased in comparison to the original DAY.

Concerning DAZ, the porous volume remained unchanged within experimental error, while the surface area decreased slightly. The NMR analyses of DAZ saturated with toluene and irradiated showed some residual VOC in the solid after irradiation. The BET results lead to the conclusion that the remaining toluene and/or oxidation products found in the DAZ after irradiation should be on the surface of the solid and not inside the structure.

3.2.2.2. Energy dispersive X-ray spectroscopy (EDS) and X-ray photoelectron spectroscopy (XPS) analyses. The results of the EDS analyses in the cases of the DAY and DAZ zeolites are shown in Table 3.

When DAY was saturated with toluene and irradiated, the ratio Si/Al decreased in comparison to the original DAY. As already observed in the NMR analyses, there was no change when DAY was irradiated in absence of pollutant. Adsorption of toluene might affect slightly the Si location in zeolite structure, as Zhu et al. have observed with a zeolite Na-Y [27]. The EDS analysis made on the DAY saturated with toluene shows also a change in the Si/Al ratio, as a consequence of the toluene adsorbed inside the zeolite which is producing a small re-arrangement in the zeolite structure, particularly in one of the Si positions [27]. However, taking into account the NMR analysis, this change occurring in the solid is not affecting in a significant way the basic structure of the solid, so any possible change in the DAY structure is mainly a consequence of the 172 nm irradiation of the toluene saturated solid. Concerning DAZ, no change could be observed in the Si/Al ratio when irradiated after saturation with toluene.

Table 3
EDS analyses of original DAY, DAY irradiated in the absence of toluene, DAY saturated with toluene and irradiated, original DAZ and DAZ saturated with toluene and irradiated at 172 nm.

Solids	Si/Al ratio
DAY	24.8 ± 0.2
DAY + $h\nu$	24.5 ± 0.2
DAY + Tol	23.0 ± 0.2
DAY + Tol + $h\nu$	19.9 ± 0.2
DAZ	15.4 ± 0.2
DAZ + Tol + $h\nu$	15.3 ± 0.2

Table 4
XPS analyses of the Si/Al ratio for original DAY, DAY irradiated in the absence of toluene, DAY saturated with toluene and irradiated, original DAZ and DAZ saturated with toluene and irradiated at 172 nm.

Solids	Si/Al analyses
DAY	6.7 ± 0.3
DAY + $h\nu$	6.6 ± 0.3
DAY + Tol	7.3 ± 0.3
DAY + Tol + $h\nu$	8.1 ± 0.3
DAZ + $h\nu$	6.4 ± 0.3
DAZ + Tol + $h\nu$	6.4 ± 0.3

Supplementary surface analyses (X-ray Photoelectron Spectroscopy, XPS) were made in order to compare the Si/Al ratio at the surface (XPS) and inside the zeolites (EDS). The results of the XPS analyses in the cases of the DAY and DAZ zeolites are shown in Table 4. They confirm that the change in the Si/Al ratio was significant in the case of the DAY zeolite saturated with toluene and irradiated.

In summary, the EDS and XPS results demonstrate that a zeolite structure rearrangement was taking place under irradiation in the presence of toluene. Some Si and Al atoms were changing their chemical characteristics and moving from their original area at the surface or in the framework of the zeolite. As already pointed out, this change was not observed without irradiation.

4. Discussion

In all the experiments described (Section 3.1), the VOC containing air stream (2000 mg m^{-3}) was continuously flushed through the reactor. For comparison, experiments were also carried out under conditions where a pure air stream was introduced in the reactor during V-UV irradiation (*i.e.* as soon as the zeolite was saturated with the VOC). Within experimental error, no significant differences were observed between the former and the latter series of experiments. This result is not surprising, taking into account the two following observations:

(i) when an air stream containing the VOC at a constant concentration of 2000 mg m^{-3} was flushed through the reactor in the absence of zeolite, in a very short time after the V-UV irradiation was started, no VOC could be detected at the reactor outlet; therefore, V-UV irradiation at 172 nm in the presence of air proved very efficient in mineralizing the VOCs in the gas phase [15–16,19];
(ii) The photo/thermodesorption phenomenon, induced by switching on the lamp, led to an important increase of the VOC concentration in the gas phase (Fig. 3); under these conditions, the amount of photons emitted by the lamp was not high enough to initiate efficiently the VOC oxidation/degradation process, thus leading to much longer mineralization times. Moreover, the intermediates in contact with the zeolite (produced during irradiation) could react at the surface, and/or diffuse inside the channels being shielded from the radiation.

The important difference in the irradiation times needed for VOC degradation in the case of toluene compare to benzene and 1-butanol may be due to basically two factors:

(i) the diffusion process through the solid and the desorption from the solid, not only of the original VOC but also of its oxidation products;
(ii) and the interaction between the VOC (and eventually its oxidation products) and the zeolite framework that might be stronger for toluene.

In fact, the π-electron system of the aromatic toluene ring interacts strongly with the Lewis acid extra-framework cation, whereas the methyl hydrogen atoms interact with the basic framework oxygen atoms [28]. This double interaction could explain the higher irradiation time required to degrade toluene, compared to benzene and 1-butanol.

Taking into account the larger porous volume of the DAY compared to DAZ, it is expected that the toluene will diffuse much better in the DAY and the CH_3 group will interact in a better way with the DAY framework. This behavior leads to different degradation pathways for the pollutant, which might affect the structural characteristics of the solid, clearly observed when the DAY was saturated with toluene and irradiated (in contrast to the DAZ).

The change in superficial and structural characteristics obtained with the DAY saturated with toluene and irradiated could be attributed to two possibilities:

(i) Some sites in the DAY zeolite are occupied by organic compounds as a result of the photolytic oxidation process of toluene or/and,
(ii) There is some intrinsic change in the zeolite which modifies the original surface characteristics.

Actually, both phenomena could occur at the same time and the oxygen molecule plays an important role in the overall oxidation process. V-UV irradiation has enough energy (695 kJ/mol at 172 nm) to cleave C–H bonds, leading directly to the formation of C-centered radicals by photolysis of the organic substrate (reaction 1)

$$RH + h\nu(172\,nm) \rightarrow R^{\bullet} + H^{\bullet} \quad (1)$$

In this case, the more labile C–H bonds in toluene are those from the CH_3 group, and V-UV irradiation of toluene leads to the production of the benzyl radical.

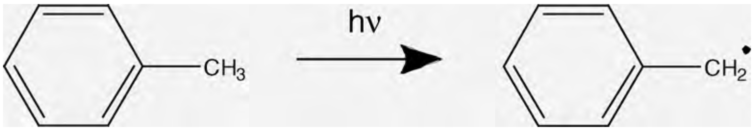

(2)

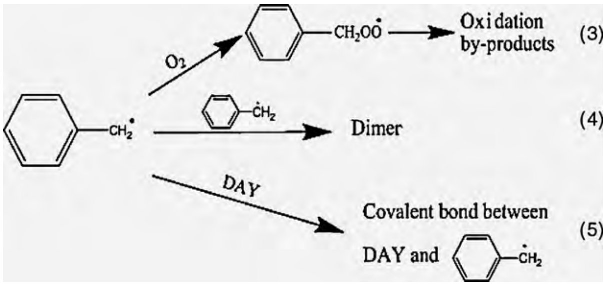

The benzyl radical may undergo several reactions. It may be trapped by molecular oxygen to yield peroxyl radicals, which are key intermediates of the subsequent thermal reactions leading to the production of by-products (*i.e.* benzaldehyde and benzoic acid) (reaction 3). These by-products could be retained in the zeolite structure or mineralized to produce CO_2 and H_2O. Another possibility is the recombination between two benzyl radicals, to form dimers (reaction 4). Moreover, benzyl radicals may react with the DAY framework (reaction 5). The possibility to produce a complex radical–zeolite has been studied by Lei et al. [29]. They reported that under appropriate conditions at room temperature, some of the radicals generated by photolysis could be persistent for a long period of time, depending on the supramolecular structure of the radical–zeolite complex and the diffusion and reaction dynamics of the radical.

In this case, the benzyl radical generated during irradiation of the DAY saturated with toluene may diffuse to the internal structure of the solid, forming a very stable complex benzyl radical–zeolite, which produces a change in the original structure of the zeolite. Apparently, this behavior is not happening with the DAZ. In the case of 1-butanol and benzene, both zeolites behave as a reservoir, where the pollutants are absorbed and later degraded by V-UV irradiation (V-UV photolysis), regenerating the adsorption capacity of the solids [15,16].

The physicochemical analyses corroborate the hypothesis of a reaction between the radical and DAY. The benzyl radical is probably bound to the Al atom of the solid structure, in agreement with the solid state NMR results, showing that changes occurred in the chemical shifts of some Al and Si atoms. In the original DAY, the Al atoms are four-coordinated and after toluene saturation and irradiation, some six-coordinated Al atoms were found, which could be attributed to the presence of a complex structure produced when the benzyl radical reacted with the zeolite framework. This reaction induced also an effect on the Si atoms shifts, which initially were in Q3 sites and after irradiation new Q4 sites were detected.

5. Conclusion

The results obtained in this work show the possibility to treat gaseous effluents containing VOCs by employing two types of zeolites as solid reservoirs (DAY and DAZ) and using V-UV irradiation at 172 nm in order to regenerate the adsorption capacity of the solids. However, important changes were detected in the structural properties of the DAY zeolite, when saturated with toluene and irradiated. These changes have been attributed to complex formation and reaction between the solid framework and the benzyl radical formed under irradiation of adsorbed toluene. In contrast, the DAZ zeolite retained its superficial and structural properties after toluene saturation and V-UV treatment. Concerning 1-butanol, changes in the DAY zeolite structure were negligible, whereas no change was detected in the case of benzene. These results could be related to two possibilities:

(i) Depending on their stability, the radicals produced during VOCs irradiation could diffuse inside the solid and react with the zeolite framework, changing its properties.
(ii) The diffusion rate of VOCs could control the efficiency of the degradation process, since the V-UV radiation at 172 nm cannot penetrate inside the zeolite and an efficient degradation of the VOC may only occur in the gas phase or at the zeolite surface.

Thus, although the combination of the adsorption process and the V-UV photolysis may be of advantage to treat pollutant containing air streams, the pollutant characteristics as well as the adsorbent properties have to be taken into account, as modification of the reservoir/adsorbent solid structure could decrease the adsorption capacity of the solid for following treatment.

Acknowledgements

The authors thank Instituto Venezolano del Petroleo (Intevep) for performing all BET, SEM and XPS analyses, and are particularly grateful to Dr. Alfredo Viloria, Luis Castillo, Ismael Gonzalez and Edgar Cañizalez from PDVSA-Intevep.

References

[1] P. Le Cloirec, Lavoisier Tec. & Doc., Paris (1998) 163–184.

[2] A.J. Teller, US Patent 6,051,199, 2000.

[3] (a) K. Hashimoto, H. Irie, A. Fujishima, Jpn. J. Appl. Phys. Part 1 44 (2005) 8269–8285;
(b) J. Mo, Y. Zhang, Q. Xu, R. Yang, J. Hazard. Mater. 168 (2009) 276–281.

[4] Y. Paz, C. R. Chim. 9 (2006) 774–787.

[5] T. Kasahara, K. Inumaru, S. Yamanaka, Micropor. Mesopor. Mater. 76 (2004) 123–130.

[6] K. Mogyoroshi, A. Farkas, I. Dekany, A. Dombi, Environ. Sci. Technol. 36 (2006) 3618–3624.

[7] J. Chen, L. Eberlein, C.H. Langford, J. Photochem. Photobiol. A: Chem. 148 (2002) 183–189.

[8] K. Inumaru, M. Murashima, T. Kasahara, S. Yamanaka, Appl. Catal. B: Environ. 52 (2004) 275–280.

[9] K. Inumaru, T. Nakano, S. Yamanaka, Micropor. Mesopor. Mater. 95 (2006) 279–285.

[10] O. Chiyoda, J. Misakab, K. Ikeue, M. Anpo, H. Yamashita, Micropor. Mesopor. Mater. 95 (2006) 279–285.

[11] P. Monneyron, M.-H. Manero, J.-N. Foussard, F. Benoit-Marquié, M.-T. Maurette, Chem. Eng. Sci. 58 (2003) 971–978.

[12] K. Yamaguchi, K. Inumaru, Y. Oumi, T. Sano, S. Yamanaka, Microp. Mesop. Mat. 117 (1–2) (2009) 350–355.

[13] Y. Kato, H. Yoshida, A. Satsuma, T. Hattori, Micropor. Mesopor. Mater. 51 (2002) 223–231.

[14] G. Yan, X. Wang, X. Fu, D. Li, Catal. Today 93–95 (2004) 851–856.

[15] P. Monneyron, A. De La Guardia, M.H. Manero, E. Oliveros, M.T. Maurette, F. Benoit-Marquié, Int. J. Photoen. 5 (2003) 167–174.

[16] P. Monneyron, Ph.D. Thesis, Institute National des Sciences Appliquées de Toulouse, 2003.

[17] L. Jakob, Ph.D. Thesis, Ecole Polytechnique Fédérale de Lausanne, 1992.

[18] L. Jakob, T.M. Hashem, S. Bürki, N.M. Guindy, A.M. Braun, J. Photochem. Photobiol. A: Chem. 75 (2) (1993) 97–103.

[19] F. Benoit-Marquié, M.T. Boisdon, A.M. Braun, E. Oliveros, M.-T. Maurette, Entropie 228 (2000) 36–43.

[20] J.M. McKelvey, H.E. Hoelscher, Anal. Chem. 29 (1) (1957) 123–132.

[21] F. Zoran, Proc. SPIE, vol. 4440, 2001, pp. 246–255.

[22] P. Monneyron, M.H. Manero, J.N. Foussard, Environ. Sci. Technol. 37 (11) (2003) 2410–2414.

[23] M. Hunger, Solid State Nuclear Magn. Reson. 6 (1996) 1–29.

[24] S. Li, S.-J. Huang, W. Shen, H. Zhang, H. Fang, A. Zheng, S.-B. Liu, F. Deng, Phys. Chem. C 112 (37) (2008) 14486–14494.

[25] C.A. Fyfe, Y. Feng, H. Grondey, G.T. Kokotailo, H. Gies, Chem. Rev. 91 (7) (1991) 1525–1543.

[26] K. Okada, N. Arimitsu, Y. Kameshima, A. Nakajima, K. MacKenzie, Appl. Clay Sci. 31 (2006) 185–194.

[27] J. Zhu, N. Trefiak, T. Woob, Y. Huang, Micropor. Mesopor. Mater. 114 (2008) 474–484.

[28] A. Simperler, R.G. Bell, A. Philippou, M.W. Anderson, J. Phys. Chem. B 106 (42) (2002) 10944–10954.

[29] X.-G. Lei, S. Jockusch, M.F. Ottaviani, N.J. Turro, Photochem. Photobiol. Sci. 2 (2003) 1095–1100.